Journal of Biomedical Research

Progressive IL-13 signaling promotes inflammation-associated liver fibrosis *via* IL-13RA2/MEK/ERK activation in *Schistosoma japonicum* infection

Ruiyan Xiong, Jiangyuan Du, Yuchen Yang, Yuxiao Zhu, Yangyue Ni, Lin Chen, Min Hou, Zhipeng Xu, Lu Chen, Minjun Ji

Cite this article as:
Ruiyan Xiong, Jiangyuan Du, Yuchen Yang, Yuxiao Zhu, Yangyue Ni, Lin Chen, Min Hou, Zhipeng Xu, Lu Chen, Minjun Ji. Progressive IL-13 signaling promotes inflammation-associated liver fibrosis *via* IL-13RA2/MEK/ERK activation in *Schistosoma japonicum* infection[J]. *Journal of Biomedical Research*, In press. doi: 10.7555/JBR.39.20250475

View online: https://doi.org/10.7555/JBR.39.20250475

Available online at www.jbr-pub.org.cn

Open Access at PubMed Central

Journal of Biomedical Research, 2026 40(0): 1–15

Original Article

JBR

Progressive IL-13 signaling promotes inflammation-associated liver fibrosis *via* IL-13RA2/MEK/ERK activation in *Schistosoma japonicum* infection

Ruiyan Xiong[1], Jiangyuan Du[1], Yuchen Yang[1], Yuxiao Zhu[1], Yangyue Ni[1], Lin Chen[1], Min Hou[1], Zhipeng Xu[1], Lu Chen[1,✉], Minjun Ji[1,2,✉]

[1]*Department of Pathogen Biology, Key Laboratory for Infections and Control of Jiangsu Province, Nanjing Medical University, Nanjing, Jiangsu 211166, China;*
[2]*Jiangsu Province Engineering Research Center of Antibody Drug, Nanjing, Jiangsu 211166, China.*

Abstract

Progressive IL-13 signaling is closely associated with liver fibrosis. Among fibrotic diseases, liver fibrosis induced by *Schistosoma japonicum* in advanced schistosomiasis is the primary driver of portal hypertension, which is the leading cause of mortality in affected patients. RNA sequencing analysis of human hepatic stellate cells revealed that *IL-13RA2* was markedly upregulated in activated hepatic stellate cells and enriched in the cytokine-receptor interaction pathways, suggesting a potential role for IL-13RA2 in hepatic stellate cell activation and fibrosis progression. Based on these findings, we aimed to investigate whether IL-13RA2 also contributes to liver fibrosis during *Schistosoma japonicum* infection. In this study, we established a murine model of *Schistosoma japonicum* infection. Compared with IL-13RA1, IL-13RA2 expression was significantly increased at week 9 post-infection in mice. IL-13RA2 was enriched within fibrotic regions and increased in parallel with collagen accumulation and stellate cell activation. The phosphorylation levels of MEK and ERK changed in parallel with IL-13RA2 abundance. Furthermore, overexpression of IL-13RA2 markedly accelerated hepatic fibrogenesis, while knockdown of IL-13RA2 attenuated liver fibrosis induced by schistosomiasis *via* the MEK/ERK pathway. Hence, IL-13RA2 may represent an effective and promising therapeutic target for the attenuation of liver fibrosis.

Keywords: *Schistosoma japonicum*, liver fibrosis, IL-13, IL-13RA2, MEK/ERK pathway

Introduction

Schistosomiasis, caused by schistosome infection, affects over 250 million people globally[1]. There are six species of *Schistosoma* that infect humans; among them, *Schistosoma japonicum* is mainly prevalent in Asia, including China, Indonesia, and the Philippines. Following egg deposition in the liver and gut, egg granulomas form and serves to sequester soluble egg antigens (SEAs), protecting adjacent tissues from damage[2]. However, sustained antigenic stimulation drives progressive fibrotic remodeling in hepatic and intestinal tissues, ultimately culminating in irreversible fibrotic damage to both the liver and the

✉Corresponding authors: Lu Chen, E-mail: chenlu8911@njmu.edu.cn, ORCID: 0000-0002-0948-6049; Minjun Ji, E-mail: jiminjun@njmu.edu.cn, ORCID: 0000-0003-0293-0255..

Received: 10 November 2025; Revised: 12 April 2026; Accepted: 18 April 2026;

CLC number: R532.21, R575.2, Document code: A

The authors reported no conflict of interests.

https://doi.org/10.7555/JBR.39.20250475

gut. Extensive liver fibrosis can result in portal hypertension, and the mortality rate in schistosomiasis patients is largely attributed to this condition[3, 4].

During the early stages of *Schistosoma japonicum* infection, from cercariae to schistosomula and finally to adult worms, the host develops a Th1-type immune response[5]. Starting from the fourth week of infection in mice, with the production of schistosome eggs, immune cells such as T cells and Kupffer cells are recruited to the eggs, and granulomas form by the fifth week[6]. Subsequently, the Th1-type immune response shifts toward the Th2-type immune response, with increased levels of cytokines such as interleukin- (IL)-13 , IL-4 and transforming growth factor beta 1 (TGF-β1). Of note, IL-13 acts as a key mediator in activating hepatic stellate cells (HSCs), directly upregulating fibrosis-related genes (*α-Sma* and *Col1a1*) and promoting the transformation into myofibroblasts[7]. In addition to IL-13, quiescent hepatic stellate cells (qHSCs) can be activated by TGF-β1 or vascular endothelial growth factor (VEGF) derived from Kupffer cells and activated HSCs, thereby promoting their transformation into myofibroblasts and exacerbating liver fibrosis[8, 9]. Therefore, IL-13 serves as the key mediator in the deterioration of liver fibrosis after schistosome infection.

IL-13 signaling occurs through two receptors, namely IL-13 receptor alpha 1 (IL-13RA1) and IL-13 receptor alpha 2 (IL-13RA2). Of these, IL-13RA2 is commonly known as a nonfunctional decoy receptor, which is typically expressed at low levels under homeostatic conditions[10]. Exposure to IL-13 or IL-4 together with IFN-γ can promote the expression of IL-13RA2[11]. Studies have demonstrated that IL-13 can activate the TGF-β promoter through IL-13RA2–mediated induction of an Activator Protein-1 (AP-1) complex containing c-Jun and Fra-2, thereby aggravating intestinal fibrosis[12]. In contrast, heightened expression of IL-13RA2 in the lung, in both its membrane-bound and soluble forms, can alleviate bleomycin-induced lung fibrosis by reducing soluble collagen and CCL17 (C-C motif chemokine ligand 17)[13]. These studies suggest that IL-13RA2 may exert distinct effects in different fibrotic processes. However, the underlying mechanisms in schistosome-induced liver fibrosis have not been fully explored.

The signaling cascade involving ERK1/2, also known as extracellular signal-regulated kinases 1 and 2, is a member of the mitogen-activated protein kinase (MAPK) family and is crucial for regulating fibrotic processes. In this signaling module, MAP2K1 and MAP2K2 (MEK1/2) act as dual-specificity kinases that phosphorylate ERK1/2, thereby activating downstream cellular responses[14]. For example, intestinal fibrosis in rats with Crohn's disease is significantly driven by the activation of p-Ras, Raf-1, MEK-1, and p-ERK1/2 in intestinal tissues[15, 16]. Similarly, in Bmi-1$^{-/-}$ mice, senescence-associated pulmonary fibrosis has been linked to TGF-β1, IL-11, MEK, and ERK[17]. In cardiac fibrosis, MEK-ERK activation mediated by GSK-3α acts as a critical profibrotic pathway in the injured heart, operating independently of the classical TGF-β1/SMAD3 axis[18]. However, the precise relationship between IL-13 and the MEK/ERK signaling pathway has not been fully elucidated.

Our results demonstrate that IL-13 aggravates liver fibrosis by activating IL-13RA2 and the MEK/ERK pathway during *Schistosoma japonicum* infection in mice and in the hepatic stellate cell line (JS1). Therefore, our findings suggest that targeting IL-13RA2 may be an effective strategy for attenuating the progression of liver fibrosis.

Materials and methods

Animals

All experimental procedures were approved by the Committee on the Ethics of Animal Experiments of Nanjing Medical University (Permit Number: IACUC-2010014) and conformed to its institutional guidelines. Mice were maintained in specific pathogen-free environments under sterile isolators, provided with autoclaved food and water, and subjected to a 12-hour light/dark cycle at a controlled temperature of 24 ℃.

Schistosoma japonicum-infected mouse models

Male C57BL/6J mice aged six weeks were each infected percutaneously with 10 ± 2 cercariae of *Schistosoma japonicum*. A control group was established consisting of uninfected mice. The overexpression negative control (OE-NC), overexpression *Il13* (OE-*Il13*), overexpression *Il13ra2* (OE-*Il13ra2*), short-hairpin negative control (shNC), and short-hairpin *Il13ra2* (sh*Il13ra2*) plasmids were injected at 2.5 mg/kg/day by dilution in 200 μL of phosphate-buffered saline (PBS), and the injections were completed rapidly within 5−8 s, twice a week. Five or six mice per group were randomly selected and sacrificed at 9 weeks post-infection. Weekly body weight measurements were conducted on the mice throughout the study.

Plasmid and adeno-associated virus serotype 8 (AAV8) construction

OE-NC, OE-*Il13*, OE-*Il13ra2*, shNC, and sh*Il13ra2* plasmids were purchased from Shanghai GenePharma Co., Ltd (Shanghai, China). AAV8-Control (a negative control AAV8) and AAV8-sh*Il13ra2* (an AAV8 targeting *Il13ra2* for silencing) were purchased from Shanghai GenePharma Co., Ltd.

Cell lines

The growth medium for the JS1 mouse hepatic stellate cell line was DMEM (Wisent, Nanjing, China), supplemented with 10% FBS (Biosharp, Guangzhou, China) and 0.1% penicillin-streptomycin (Biosharp), and cultured under constant conditions at 37 ℃ with 5% CO_2.

JS1 cells were seeded into culture plates and allowed to reach an appropriate cell density prior to treatment. For cytokine stimulation assays, cells were exposed to recombinant IL-13 at 0, 2, 10, or 50 ng/mL, with or without the addition of TGF-β1 (5 ng/mL). Cells were collected after 24 h for RNA extraction and after 48 h for protein analysis. For transient transfection experiments, cells were transfected with OE-NC, OE-*Il13ra2*, shNC, or sh*Il13ra2* plasmids using Lipofectamine 3 000 (Invitrogen, Carlsbad, CA, USA) according to the manufacturer's instructions. After 6–8 h, the transfection mixture was replaced with fresh complete medium. Subsequently, cells were stimulated with IL-13 (10 ng/mL) for 24 h for RNA analysis or 48 h for protein analysis.

RNA extraction and quantitative PCR analysis

According to the detailed instructions from the manufacturer, total RNA was extracted from mouse livers or cell cultures using RNAiso Plus kits (Vazyme, Nanjing, China). The PrimeScript RT Master Mix kits (Vazyme) were used to synthesize first-strand cDNA from the mRNA. Quantitative real-time PCR was performed using the LightCycler® Real-Time PCR System (Roche, Basel, Switzerland) with ChamQ Blue Universal SYBR qPCR Master Mix (Cwbio, Taizhou, China). The qPCR reaction program was set based on a predefined protocol. Relative transcript levels were assessed using the $2^{-\Delta\Delta ct}$ method. The specific primer sequences are listed in ***Supplementary Table 1***.

Western blot analysis

Mouse livers were dissected, and liver specimens, together with JS1 cells, were immediately lysed in RIPA buffer (Beyotime, Shanghai, China) containing protease and phosphatase inhibitors cocktails (Beyotime) for protein extraction. The cell lysates were denatured by boiling in SDS sample buffer for 5 min. Proteins were then separated by SDS-polyacrylamide gel electrophoresis and transferred to PVDF membranes, which were then blocked at room temperature for 2 h with of 5% nonfat dry milk in PBS-Tween. Thereafter, the membranes were incubated overnight at 4 °C with primary antibodies directed at specific targets: GAPDH (1:5 000, Cat. #AF7021, Affinity Biosciences, Jiangsu, China), IL-13RA2 (1:800, Cat. #11059-1-AP, Proteintech Group, Wuhan, Hubei, China), p-MEK1/2 (1:1 000, Cat. #AF8035, Affinity Biosciences), MEK1/2 (1:1 000, Cat. #AF6385, Affinity Biosciences), p-ERK1/2 (1:1 000, Cat. #AF1015, Affinity Biosciences), and ERK1/2 (1:1 000, Cat. #AF0155, Affinity Biosciences), followed by incubation for 2 h with anti-rabbit (1:5 000, Cat. S0010, Affinity Biosciences) or anti-mouse (1:10 000, Cat. S0002, Affinity Biosciences) secondary antibodies. Immunoreactive bands were visualized using an ultrasensitive chemiluminescence imaging system with enhanced chemiluminescence (ECL) substrate (Beyotime). Band intensity was measured using Image Lab 6.0 software.

RNA-sequencing (RNA seq) analysis

Control mice and mice at 9 weeks post-infection were euthanized, and liver tissue samples (50–100 mg) were rapidly frozen in liquid nitrogen and stored at −80 ℃. Total RNA was then isolated, and sequencing libraries were prepared and sequenced by Majorbio Bio-Pharm (Shanghai, China). To identify differentially expressed genes, we used the EdgeR software to compare expression profiles between groups. Genes with an absolute $|\log_2(\text{fold change})| \geq 1$ with P-value < 0.05 were considered significantly differentially expressed. In addition, a publicly available RNA-seq dataset related to growing and senescent human activated hepatic stellate cells (GSE11954) was downloaded from the GEO database for further comparative analysis.

Histology and immunohistochemistry analyses

After fixation in 4% paraformaldehyde, mouse livers were embedded in paraffin and sliced into 4-μm-thick sections. For retrieve antigens, the slides were treated with a 10 mmol/L sodium citrate solution (pH 6.0) and boiled for 15 min. Endogenous

peroxidase activity was blocked with 3% H_2O_2, and nonspecific binding was blocked using a blocking reagent (Beyotime). The sections were incubated at 4 ℃ overnight with anti-IL-13RA1 (1:100, Cat. #AF9095, Affinity Biosciences), anti-IL-13RA2 (1:100, Cat. #11059-1-AP, Proteintech Group) and anti-IL-4RA (1:100, Cat. #DF8567, Affinity Biosciences). An HRP-conjugated goat anti-rabbit IgG (H+L) secondary antibody was used. Chromogenic signal was developed with DAB substrate, and images were obtained using a light microscope (Carl Zeiss, Germany).

Hematoxylin–eosin (H&E) and Masson staining

Liver tissue specimens embedded in paraffin underwent H&E and Masson's trichrome staining. All staining procedures were performed by a commercial histopathology service provider (Servicebio, Wuhan, China) using standardized protocols. After staining, liver inflammation and fibrosis were evaluated under a light microscope.

Immunofluorescence analysis

According to previous methods, after fixation and blocking, the liver sections were incubated for overnight at 4 ℃ with the following primary antibodies: α-SMA (1:200, Cat. #BF9212, Affinity Biosciences) and IL-13RA2 (1:150, Cat. #11059-1-AP, Proteintech Group). Following a one-hour room temperature with species-matched secondary antibodies, cell nuclei were counterstained with DAPI for 3 min prior to imaging.

Statistical analysis

Analyses were performed using GraphPad Prism 9.0. Data were presented as mean ± standard error of the mean (SEM) based on at least three independent experiments. Differences between two groups were analyzed using the Student's *t*-test, while one-way ANOVA with Bonferroni post hoc test was used for multiple group comparisons. Statistical significance was defined as P values < 0.05.

Results

IL-13RA2 is markedly upregulated in activated human hepatic stellate cells

In an RNA-seq comparison of quiescent and activated HSCs (GSE11954), the cytokine–receptor interaction pathway was significantly enriched (***Fig. 1A***). Among the differentially expressed genes, *IL-13RA2* showed marked upregulation, along with increased *TGF-β* expression (***Fig. 1B–1D***), suggesting a potential role in the fibrogenic activation of HSCs. Considering that excessive HSC activation underlies hepatic fibrosis, we next examined whether IL-13RA2 exerts a similar profibrotic role during *Schistosoma japonicum* infection.

Schistosoma japonicum infection enhances type 2 immunity-related cytokines and aggravated liver fibrosis

Mice were infected with *Schistosoma japonicum*

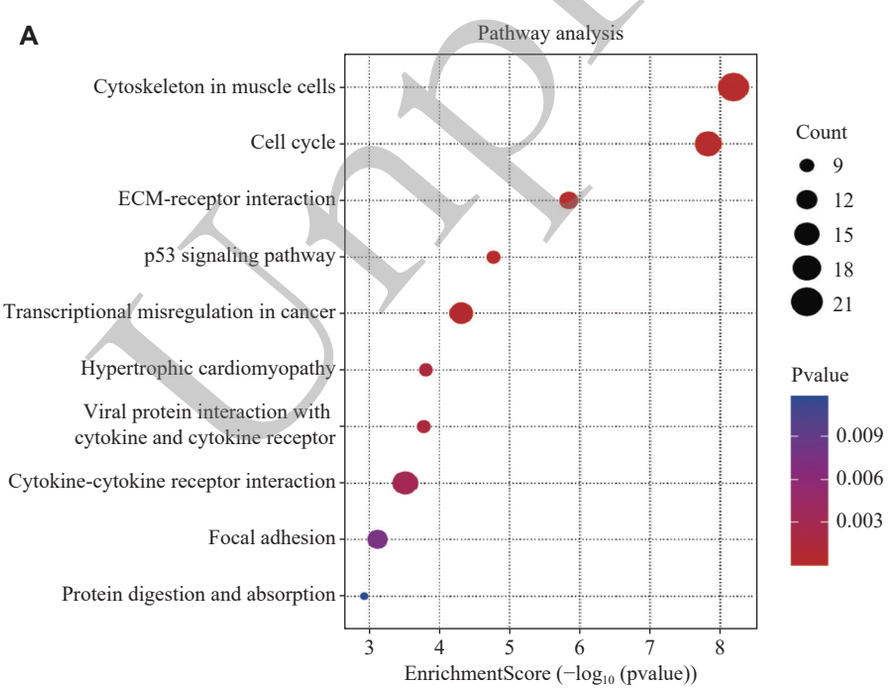

(Continued)

(Continued)

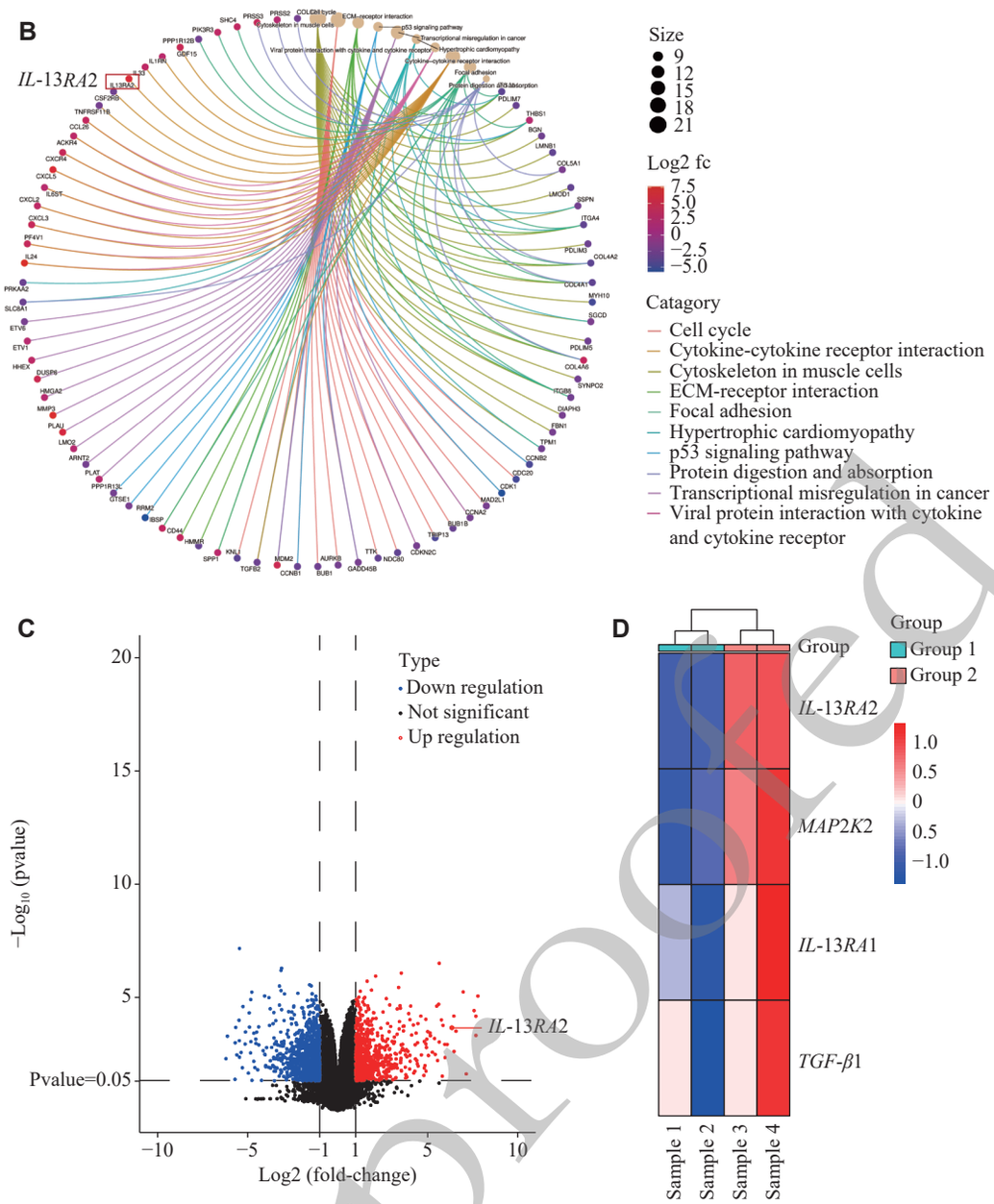

Fig. 1 **IL-13RA2 is markedly upregulated in activated human hepatic stellate cells (HSCs)** A: Top 10 enriched Kyoto Encyclopedia of Genes and Genomes (KEGG) pathways identified in human HSCs (GSE11954). B: Circular plot showing KEGG pathway enrichment analysis for differentially expressed genes (DEGs) in growing versus quiescent human HSCs. C: Volcano map of the DEGs between growing and senescent activated HSCs. The x-axis illustrates the $\log_2$(fold change [FC]), and the y-axis showing the *P* value. Data points in red represent genes that are considerably enhanced ($\log_2$FC > 1, $P < 0.05$). Data points in blue represent genes that are significantly downregulated ($\log_2$FC < −1, $P < 0.05$), and non-important genes are shown in gray. D: Heat map analysis of *IL-13RA1*, *IL-13RA2*, *TGF-β1*, and *MAP2K2* mRNA expression between senescent (Group 1: Samples 1 and 2) and growing (Group 2: Samples 3 and 4) HSCs.

for 0, 6 or 9 weeks, respectively. At week 6 and 9 after infection, prominant granulomas were observed by H&E staining, accompanied by hepatocyte necrosis around the eggs in the liver (***Fig. 2A*** and ***2D***). Meanwhile, Masson staining revealed extensive collagen deposition compared with week 0, along with destruction of the liver lobular structure (***Fig. 2B*** and ***2E***). Immunohistochemical staining revealed increased expression of α-SMA (alpha-smooth muscle actin), a marker of activated myofibroblasts, indicating enhanced fibrotic activity at both time points (***Fig. 2C*** and ***2F***). In addition, the expression of *Acta2* and *Col1a1* were both significantly increased in the liver at both week 6 and week 9 after *Schistosoma japonicum* infection (***Fig. 2G*** and ***2H***).

We then assessed the mRNA expression levels of *Il4*, *Il13*, and *Tgfb* in the liver in mice at the week 6

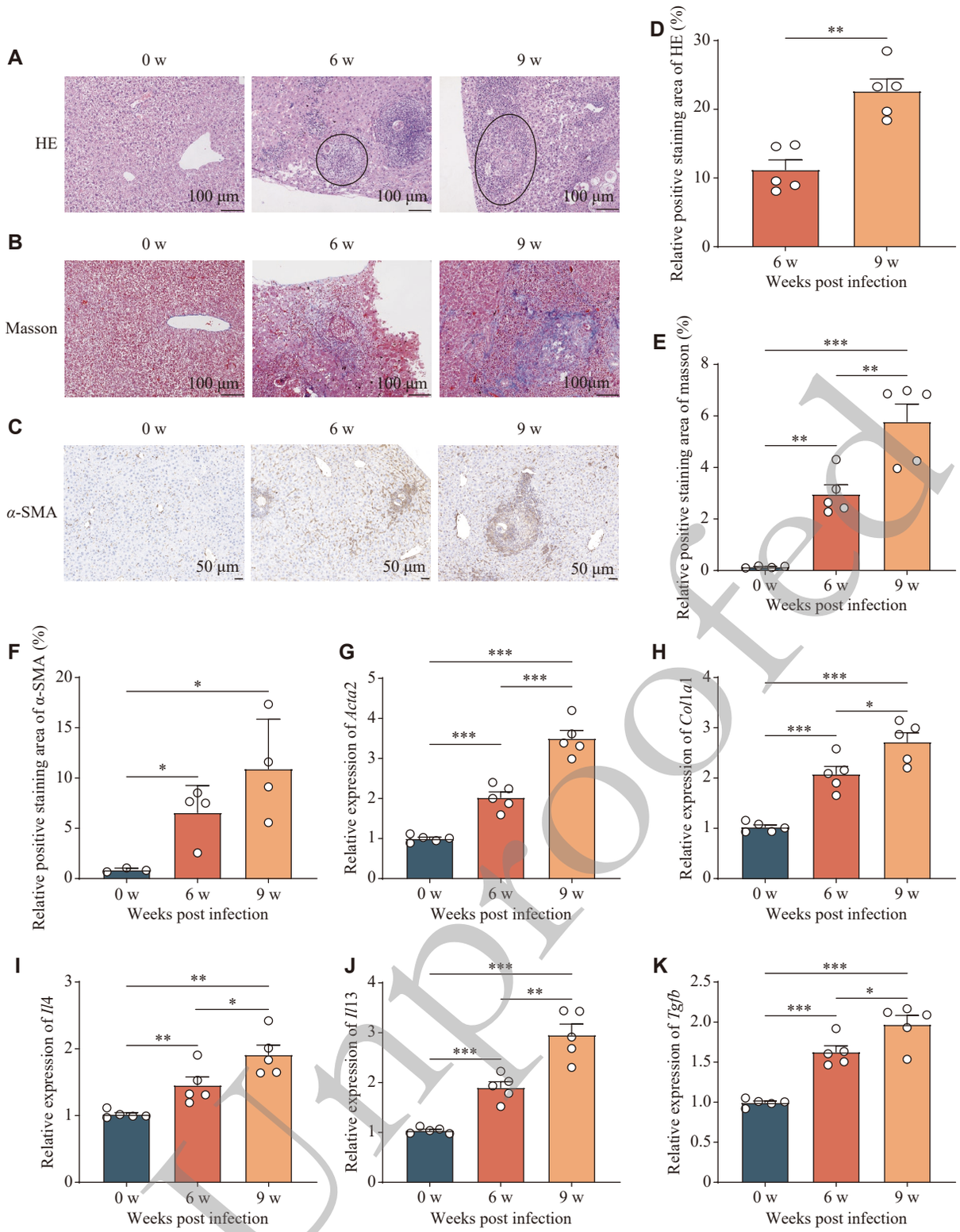

***Fig. 2 Schistosoma japonicum* infection enhances type 2 immunity-related cytokines and aggravates liver fibrosis** A: Representative images of hematoxylin–eosin (H&E) staining of liver sections from mice at week 0, week 6, and week 9 post-infection. B: Masson's trichrome staining. C: Immunohistochemical (IHC) detection of α-SMA. D–F: Quantification of statistical analysis for H&E (D), Masson (E), and α-SMA IHC staining (F). G–K: qRT-PCR analysis of *Acta2* (G), *Col1a1* (H) mRNA expression, and type 2 cytokines *Il4* (I), *Il13* (J), and *Tgfb1* (K) expression in liver tissues of mice. Data are presented as mean ± standard error of the mean (One-way ANOVA with Bonferroni post hoc test). $^{*}P < 0.05$; $^{**}P < 0.01$; $^{***}P < 0.001$. $n = 5$ per group. Scale bars: A and B, 100 μm; C, 50 μm.

and week 9 post-infection. The expression of *Il4* (***Fig. 2I***), *Il13* (***Fig. 2J***), and *Tgfb* (***Fig. 2K***) was higher at week 9 than week 6, and *Il13* showing the most pronounced upregulation (***Fig. 2J***).

Schistosoma japonicum infection promotes the expression of IL-4 and IL-13-related receptors, particularly increased the expression of IL-13RA2

To investigate the temporal gene expression changes during *Schistosoma japonicum* infection, RNA-seq was performed on livers from control mice and mice at 9 weeks post-infection. A total of 2 984 genes were found to be upregulated, and 1 475 genes were downregulated in the differential expression analysis (***Fig. 3A***). The Kyoto Encyclopedia of Genes and Genomes (KEGG) pathway enrichment analysis demonstrated significant enrichment of the

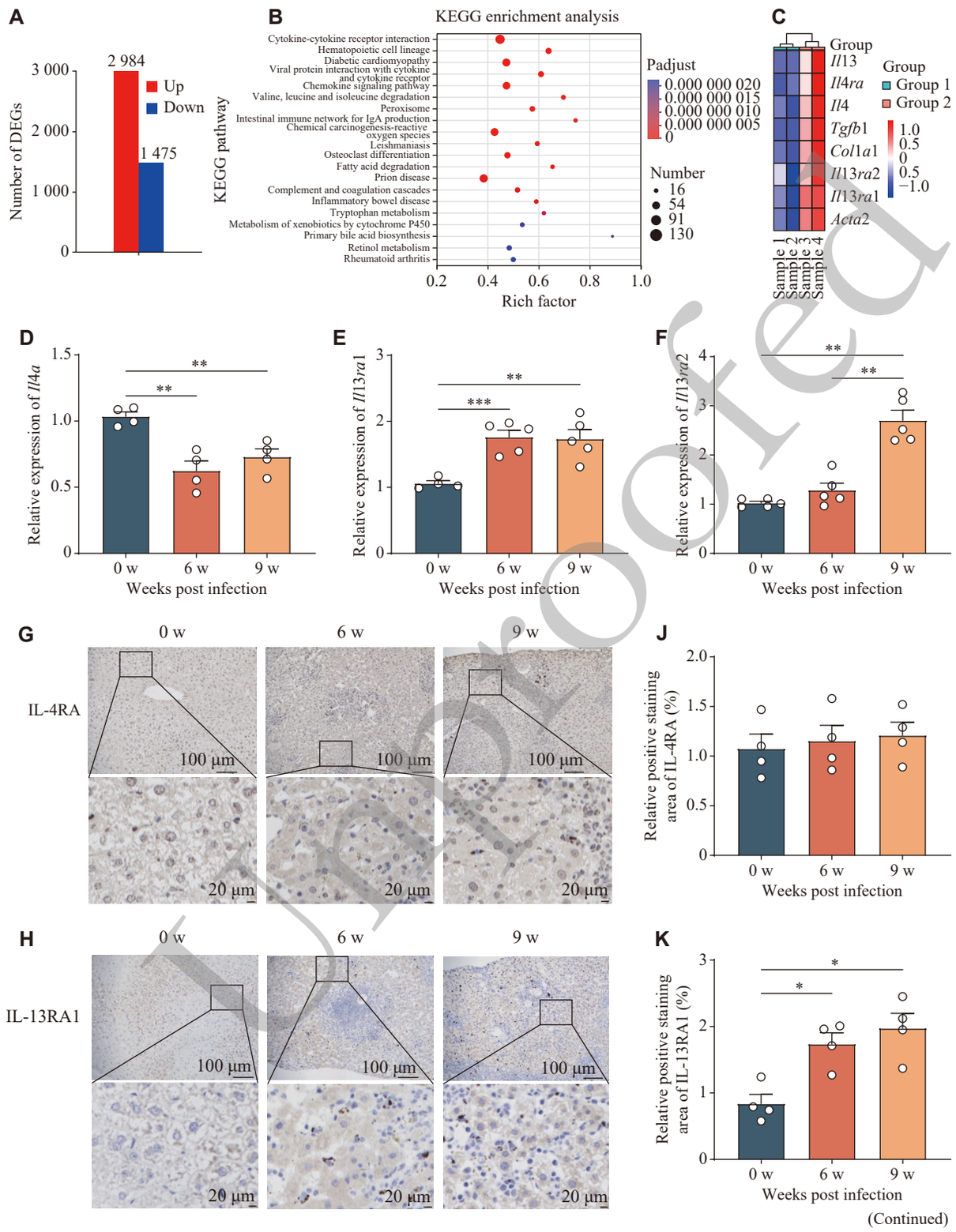

(Continued)

(Continued)

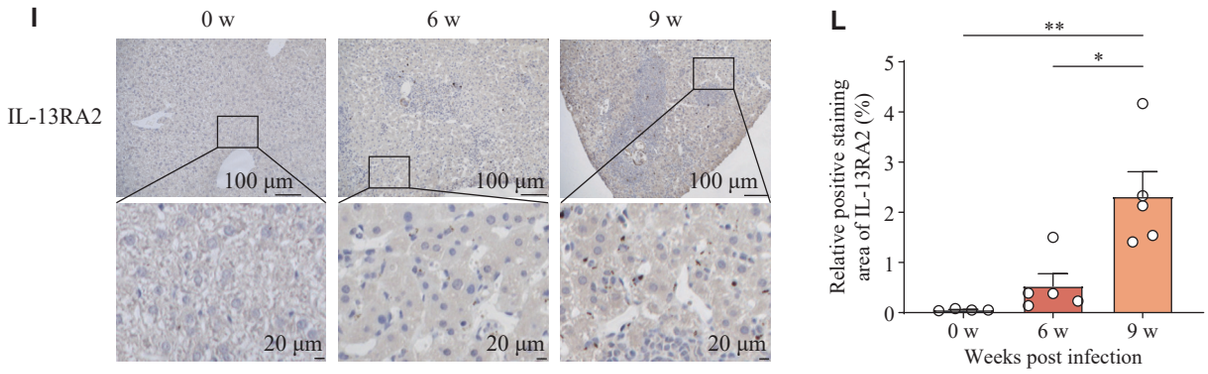

***Fig. 3 Schistosoma japonicum* infection promotes the expression of IL-4 and IL-13-related receptors, particularly increases the expression of IL-13RA2** A. Number of differentially expressed genes (DEGs) in liver tissues of mice at week 9 post-infection compared with controls. B. Top 20 enriched pathways identified in liver tissues of mice at week 9 post-infection compared with controls. C. Heatmap illustrating the expression patterns of representative DEGs in liver tissues of control mice (Group 1: Samples 1 and 2) and *Schistosoma japonicum*-infected mice (Group 2: Samples 3 and 4) at week 9 post-infection . D–F: Quantitative RT-qPCR analysis of *Il4ra* (D), *Il13ra1* (E) and *Il13ra2* (F) expression levels in liver tissues of mice. G–I: Representative immunohistochemical images of liver IL-4RA (G), IL-13RA1 (H) and IL-13RA2 (I) in liver tissues of mice. J–L: Quantification immunohistochemical staining for IL-4RA (J), IL-13RA1 (K), and IL-13RA2 (L) in liver tissues of mice. Data are presented as mean ± standard error of the mean (One-way ANOVA with Bonferroni post hoc test). $^{*}P < 0.05$; $^{**}P < 0.01$; $^{***}P < 0.001$. $n = 5$ per group. Scale bars: G–I, 100 μm; enlarged views, 20 μm.

cytokine–cytokine receptor interaction pathway (***Fig. 3B***). Key fibrogenic mediators including *Il13*, *Il13ra1*, *Il13ra2*, *Tgfb1*, *Acta2*, and *Col1a1* were markedly increased in the infected mice (***Fig. 3C***). We further examined the expression of *Il4ra*, *Il13ra1*, and *Il13ra2*. *Il4ra* expression decreased throughout the infection, while *Il13ra1* increased at week 6 and week 9. *Il13ra2* expression did not significant increase at week 6 but was markedly elevated at week 9 (***Fig. 3D–3F***). These data suggest that sharp upregulation of IL-13RA2 at the later stage of infection may indicate its involvement in the liver fibrosis process during schistosomiasis, prompting us to further investigation of its functional role.

IL-13/IL-13RA2 overexpression aggravates *Schistosoma japonicum*-induced liver fibrosis

To examine how IL-13 and IL-13RA2 are involved in liver fibrosis resulting from *Schistosoma japonicum*, mice were injected with overexpression plasmids of negative control (OE-NC), *IL-13* (OE-*IL-13*),and *IL-13RA2* (OE-*IL-13RA2*) as well as shRNA of negative control (shNC) and *IL-13RA2* (sh*IL-13RA2*), respectively, from weeks 5 to 9 post-infection.. As shown in ***Fig. 4A–4B***, the expression of IL-13 and IL-13RA2 was significantly increased in the OE-*Il13* and OE-*Il13ra2* groups, while the *Il13ra2* levels were reduced in the sh*Il13ra2* group compared with the negative control groups.

Overexpression of *Il13* and *Il13ra2* led to increased liver weight (***Fig. 4D***), accompanied by increased collagen deposition, a higher collagen area ratio, more severe fiber hyperplasia (***Fig. 4E–4H***), and significantly elevated expression of *Acta2* and *Col1a1* (***Fig. 4I*** and ***4J***). In contrast, knockdown of *Il13ra2* resulted in reduced collagen deposition, a decreased collagen area ratio (***Fig. 4E–4H***), and lower mRNA expression of *Acta2* and *Col1a1* (***Fig. 4I*** and ***4J***). Consistently, AAV-mediated knockdown of *Il13ra2* in *Schistosoma japonicum*-infected mice also resulted in improved hepatic histopathology and reduced collagen accumulation in the liver (***Supplementary Fig. 1A***). These results indicate a pro-fibrotic role for IL-13/IL-13RA2 signaling.

Liver fibrosis is significantly influenced by the IL-13/IL-13RA2/MEK/ERK signaling pathway

To further explore how IL-13/IL-13RA2 are involved in liver fibrosis, we used the UCSC Gene Interactions tool to identify interacting proteins. We found that MAP2K1 and MAP2K2 interact with IL-13RA2 (***Fig. 5A***). Given the well-established role of the MEK/ERK pathway in mediating inflammatory and fibrotic responses, this finding led us to hypothesize that IL-13RA2 might exert its profibrotic effects, at least in part, through activation of this pathway.

In the livers of mice infected with *Schistosoma japonicum* at weeks 0, 6, and 9, the expression of both *Map2k1* and *Map2k2* was significantly increased at week 9 (***Fig. 5B*** and ***5C***). Moreover, *Il13* and *Il13ra2* overexpression promoted the phosphorylation of MEK1/2 (p-MEK1/2) and the phosphorylation of ERK1/2 (p-ERK1/2), whereas p-MEK1/2 and p-

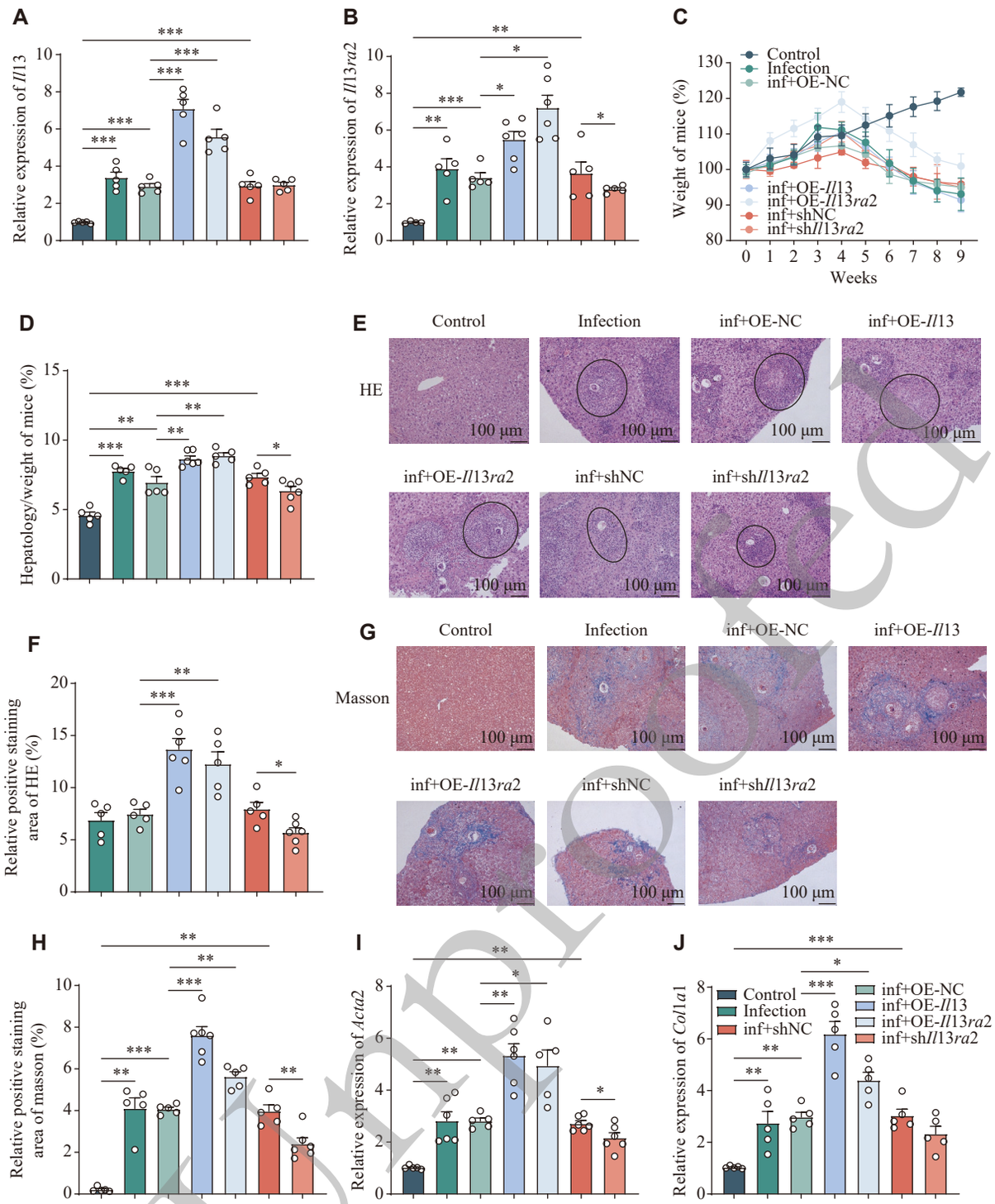

Fig. 4 **IL-13/IL-13RA2 overexpression aggravates *Schistosoma japonicum*-induced liver fibrosis** Mice were assigned to uninfected control, infected OE-NC, OE-*Il13*, OE-*Il13ra2*, shNC, and sh*Il13ra2* groups. A: *Il13* mRNA expression in the liver. B: *Il13ra2* mRNA expression in the liver. C: Body weight change of mice. D: Liver weight-to-body weight ratio of mice. E and F: Representative hematoxylin–eosin (H&E) staining images (E) and its quantification (F) of mouse liver. G and H: Representative Masson staining images (G) and its quantification (H) of mouse liver. I and J: Liver mRNA expression of *Acta2* (I) and *Col1a1* (J). Data are presented as mean ± standard error of the mean (One-way ANOVA with Bonferroni post hoc test). $^{*}P < 0.05$; $^{**}P < 0.01$; $^{***}P < 0.001$. $n = 6$ per group. Scale bars: E and G, 100 μm. Abbreviations: inf+OE-NC, infected mice transfected with the overexpression negative control plasmid; inf+OE-*Il13*, infected mice transfected with the Il13 overexpression plasmid; inf+OE-*Il13ra2*, infected mice transfected with the *Il13ra2* overexpression plasmid; inf+shNC, infected mice transfected with the short-hairpin negative control plasmid; Inf+sh*Il13ra2*, infected mice transfected with the sh*Il13ra2* plasmid.

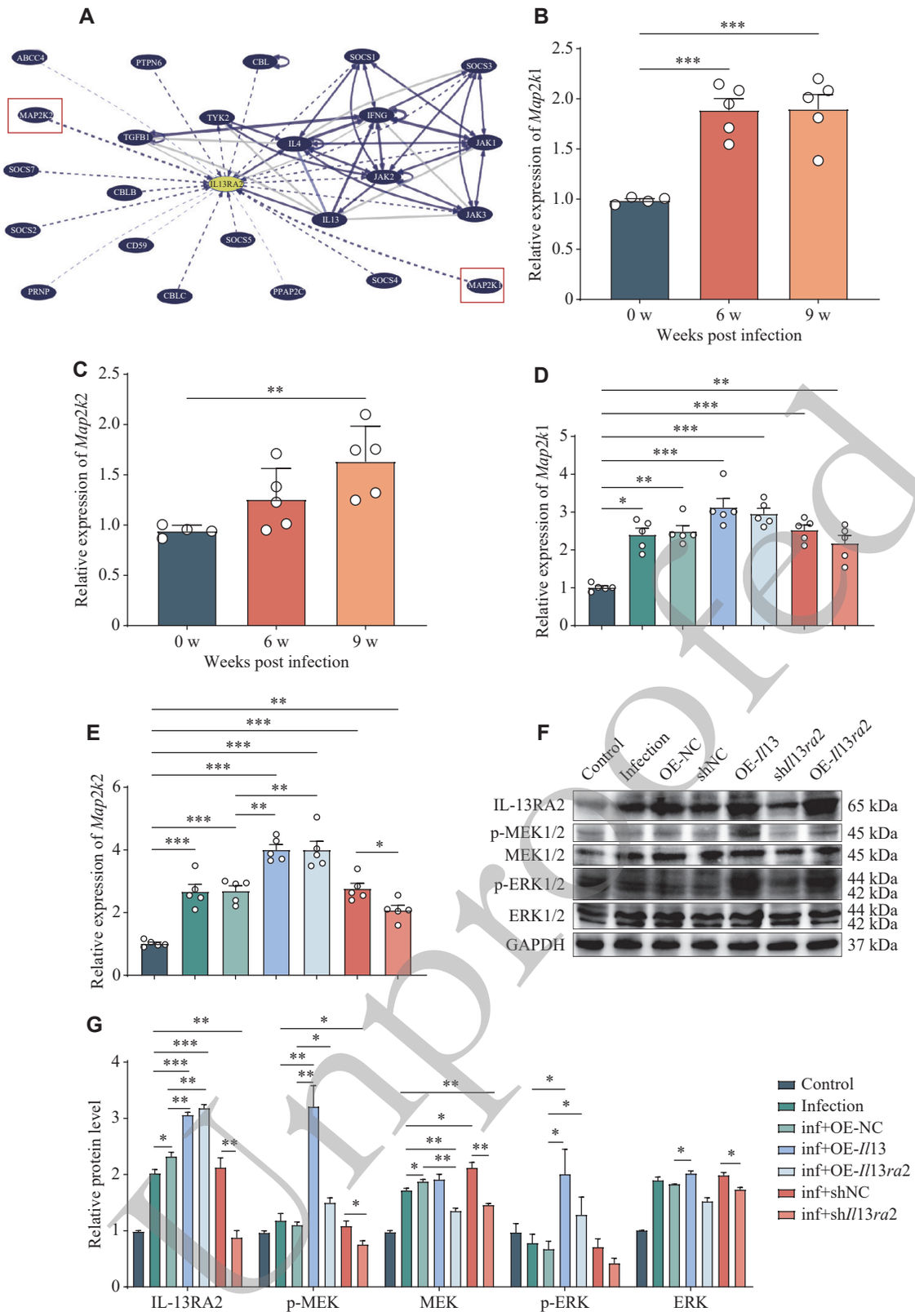

Fig. 5 **Liver fibrosis is significantly influenced by the IL-13/IL-13RA2/MEK/ERK signaling pathway** A: Predicted protein interactions between IL-13RA2 and MAP2K1 and MAP2K2. B and C: *Map2k1* (B) and *Map2k2* (C) mRNA expression in mouse liver at 0, 6 and 9 weeks after *Schistosoma japonicum* infection. D and E: *Map2k1* (D) and *Map2k2* (E) mRNA expression in the liver of mice injected with plasmid and infected with *Schistosoma japonicum* for 9 weeks. F: Expression of IL-13RA2, p-MEK1/2, MEK1/2, p-ERK1/2 and ERK1/2 in the liver of mice, detected by Western blot analysis. G: Quantification of IL-13RA2, p-MEK, MEK, p-ERK, and ERK protein expression levels by Western blot, normalized to GAPDH. Data are presented as mean ± standard error of the mean (One-way ANOVA with Bonferroni post hoc test). $^{*}P < 0.05$; $^{**}P < 0.01$; $^{***}P < 0.001$. $n = 5$ per group.

ERK1/2 levels were reduced following sh*Il13ra2* plasmid injection (***Fig. 5D–5G***).

Activation of IL-13RA2/MEK/ERK pathway in HSCs promotes liver fibrosis

Activated hepatic stellate cells are fundamentally involved in liver fibrosis. Therefore, we investigated whether IL-13RA2 in HSCs promotes liver fibrosis. Immunofluorescence staining showed that IL-13RA2 and α-SMA exhibited stronger fluorescence in the OE-*Il13* and OE-*Il13ra2* plasmid-injected groups after *Schistosoma japonicum* infection, while the sh*Il13ra2* treatment group exhibited weaker fluorescence (***Fig. 6A***). Furthermore, AAV-mediated *Il13ra2* knockdown in the liver significantly reduced liver fibrosis and α-SMA expression. (***Supplementary Fig. 1B***).

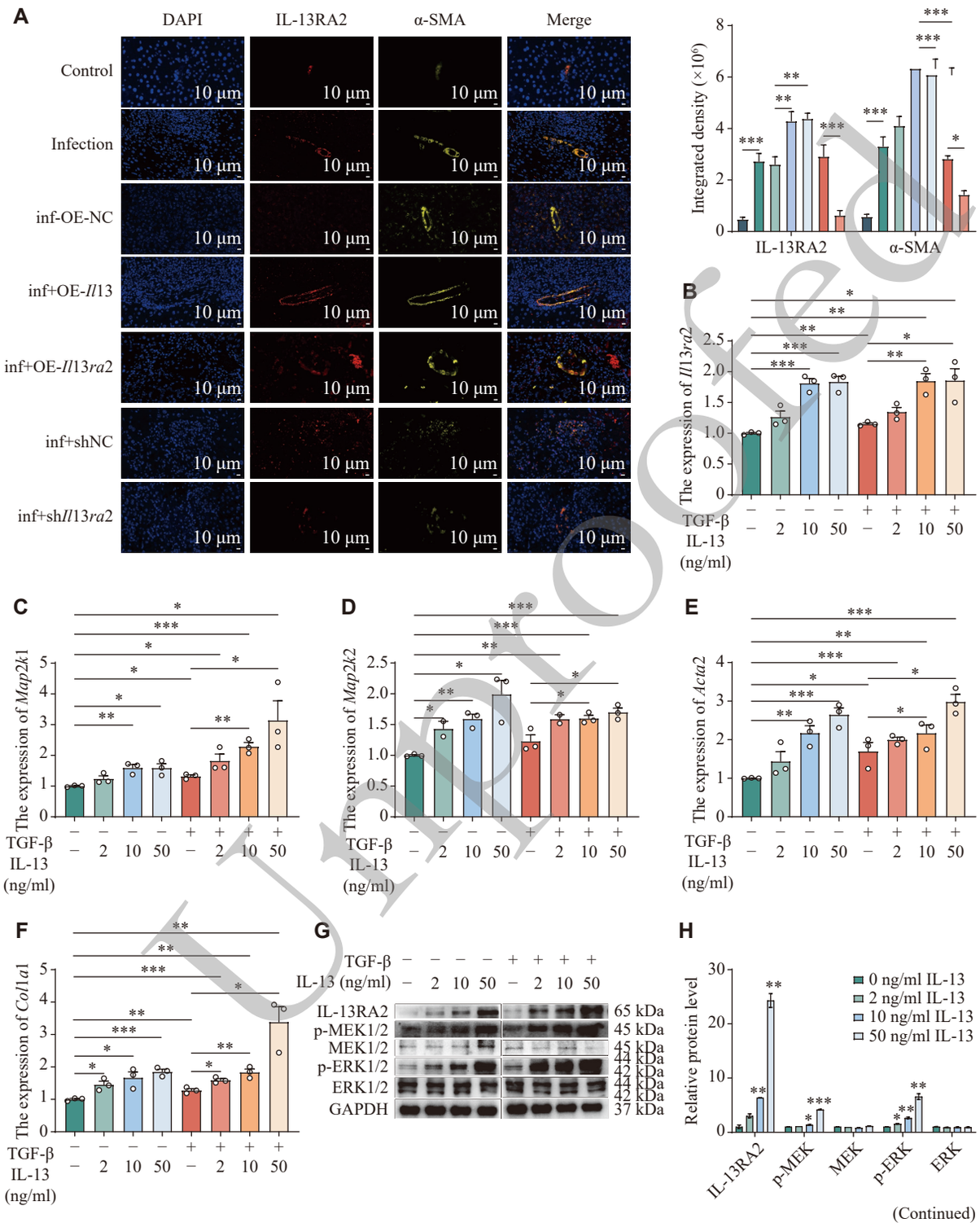

(Continued)

(Continued)

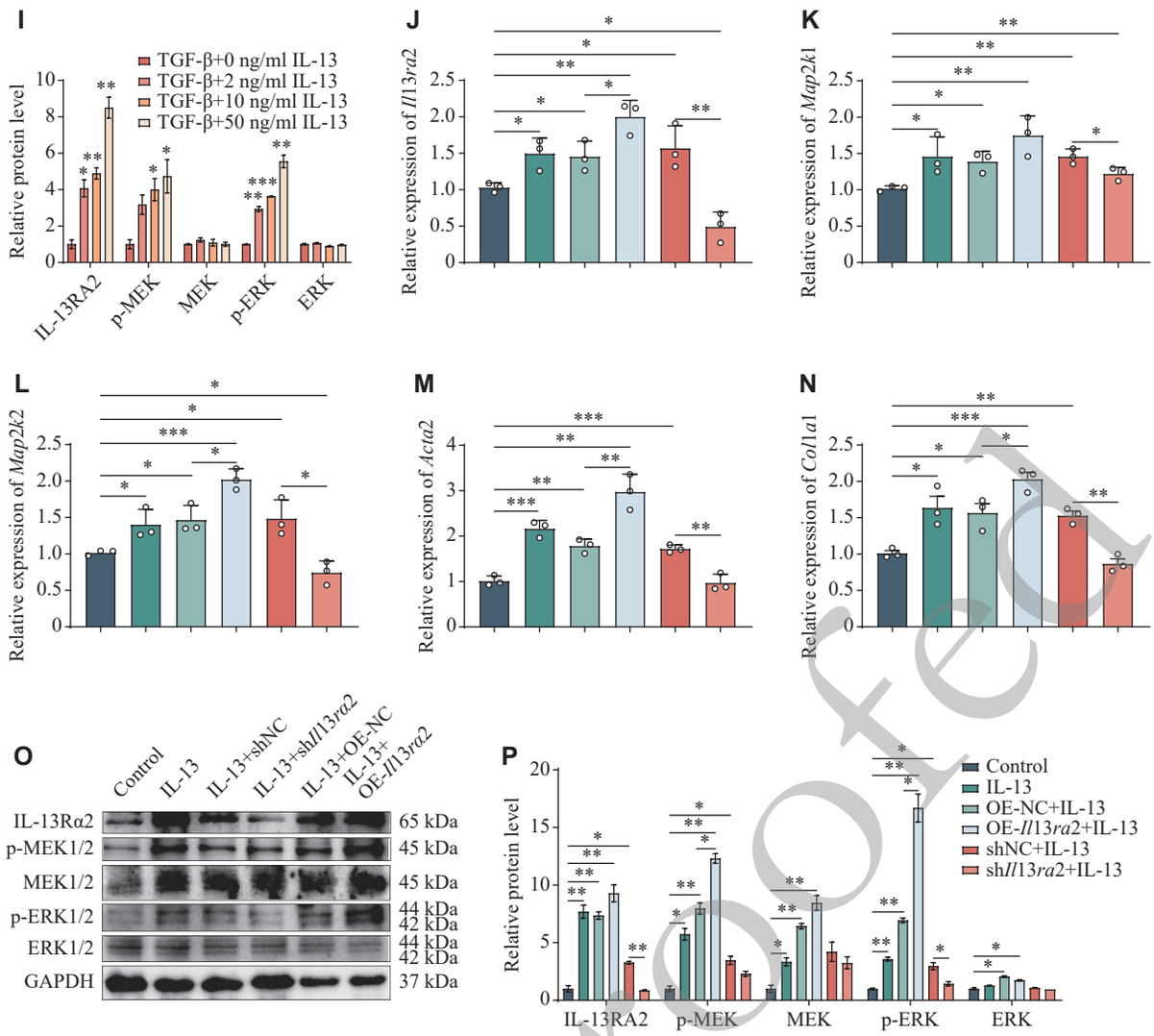

Fig. 6 **Activation of IL-13RA2/MEK/ERK pathway in human hepatic stellate cells (HSCs) promotes liver fibrosis** A: Representative images of IL-13RA2 and α-SMA immunofluorescence staining in liver sections of mice from each group. B–F: JS1 cells were stimulated with different concentrations of IL-13 (0, 2, 10, 50 ng/mL), with or without TGF-β (5 ng/mL) for 24 h. The mRNA expressions of *Il13ra2* (B), *Map2k1* (C), *Map2k2* (D), *Acta2* (E), and *Col1a1* (F) was determined by RT-qPCR. G–I: Protein expression and quantification of IL-13RA2, p-MEK1/2, MEK1/2, p-ERK1/2, and ERK1/2 in JS1 cells was detected by western blot, normalized to GAPDH. J–N: *Il-13ra2* was knocked down or overexpressed on the JS1 cell line, and stimulated with IL-13 (10 ng/mL) on the JS1 cell line for 24 h. The mRNA expressions of *Il13ra2* (J), *Map2k1* (K), *Map2k2* (L), *Acta2* (M) and *Col1a1* (N) was determined using RT-qPCR. O and P: Protein expression and quantification of IL-13RA2, p-MEK1/2, MEK1/2, p-ERK1/2, and ERK1/2 was detected by western blot, normalized to GAPDH. Data are presented as mean ± standard error of the mean (One-way ANOVA with Bonferroni post hoc test). $^{*}P < 0.05$; $^{**}P < 0.01$; $^{***}P < 0.001$. $n = 3$ per group. Scale bars: A, 10 μm.

Consistently, a heatmap of mouse liver samples showed that AAV-mediated *Il13ra2* knockdown also led to decreased expression of *Acta2* and *Col1a1* (***Supplementary Fig. 1C***).

To clarify whether the IL-13RA2/MEK/ERK pathway activated by IL-13 requires TGF-β, we stimulated JS1 cells with varying concentrations (0, 2, 10, 50 ng/mL) of IL-13 with or without TGF-β (5 ng/mL) for 24 hours. IL-13 alone (10 and 50 ng/mL) upregulated IL-13RA2 and activated p-MEK1/2 and p-ERK1/2 (***Fig. 6B*** and ***6G-I***), with corresponding increases in *Map2k1* (***Fig. 6C***), *Map2k2* (***Fig. 6D***), *Acta2* (***Fig. 6E***), and *Col1a1* (***Fig. 6F***, ***Supplementary Fig. 2A–2C***). TGF-β further enhanced this activation. These results demonstrate that IL-13 synergizes with TGF-β to promote HSC activation, and IL-13 alone is sufficient to activate the IL-13RA2/MEK/ERK pathway and drive HSC activation.

Based on the above results, *Il13ra2* was overexpressed or knocked down in JS1 cells (***Fig. 6J***), followed by IL-13 (10 ng/mL) stimulation for 24 hours. After overexpressing *Il13ra2* and stimulating

with IL-13, the expression of p-MEK, p-ERK, α-SMA, and COL1A1 significantly increased, whereas knockdown of *Il13ra2* reduced their expression (***Fig. 6K–6P***, ***Supplementary Fig. 2D*** and ***2E***). These results confirm a positive correlation between IL-13RA2 and p-MEK/p-ERK, indicating that activation of the IL-13RA2/MEK/ERK pathway promotes fibrosis.

Discussion

Parasitic diseases, such as schistosomiasis, are major contributors to liver fibrosis, often leading to ascites, splenomegaly, esophageal variceal bleeding, portal hypertension, and even death[19, 20]. Therefore, identifying critical molecular targets and developing effective anti-fibrotic therapies following schistosomiasis infection are of significant importance for improving quality of life.

Type 2 immunity, an important immune response in both mouse and humans with schistosomiasis, acts as a protective response during infection. The existence of eggs in the liver triggers a type 2 cytokine response; IL-4 and IL-13 directly or indirectly coordinate tissue repair by targeting macrophages or HSCs[21, 22]. They can promote macrophage polarization into M2 phenotype, which suppresses the IL-12/Th1/M1 response and IL-17-mediated neutrophil recruitment, ultimately facilitating tissue repair and maintaining intestinal barrier integrity[23]. However, chronic and persistent activation of type 2 immunity leads to excessive HSC activation. Activated HSCs produce collagen fibers and drive granulomas to isolate egg antigens, resulting in fibrosis. Although IL-4 and IL-13 are both critical in type 2 responses, accumulating evidence suggests that IL-13 exerts a more prominent influence in the progression of fibrosis[24, 25]. IL-13 is highly upregulated in schistosomiasis-induced liver fibrosis, and its inhibition reduces granuloma formation and improves survival in mice[26]. Similarly, blocking IL-13 reduces fibrosis and collagen deposition in pulmonary fibrosis models[27]. Other studies have also shown that inhibiting IL-13/IL-4 signaling may serve as a therapeutic target for the treatment of fibrosis[28]. Given this evidence, targeting the IL-13/IL-4 axis has emerged as a potential antifibrotic strategy. Our findings indicate that liver fibrosis triggered by *Schistosoma japonicum* also exhibits persistent type 2 immune activation, with IL-13 significantly exacerbating granuloma formation and fibrosis progression.

IL-13 binds to two receptors, IL-13RA1 and IL-13RA2. IL-4RA forms a type I IL-4 receptor with γc, and its heterodimerization with IL-13RA1 results in a type II IL-4 receptor, which also functions as an IL-13 receptor complex[29]. Previous studies have primarily focused on IL-13RA1 and IL-4RA in the context of fibrosis. It has been reported that *Il4rα* knockout mice infected with *Schistosomiasis mansoni* exhibited acute schistosomiasis but controlled liver fibrosis[30]. Similarly, systemic or macrophage-specific *Il4rα* knockout in mice resulted in inhibited liver fibrosis[31]. Furthermore, gene correlation analysis of human white adipose tissue samples also showed a strong positive correlation between fibrosis and IL-13/IL-4RA signaling[22]. IL-13RA1 and the transcription factor STAT6 aggravate liver fibrosis through a TGF-β-dependent pathway by releasing osteoprotegerin (OPG), suggesting that IL-4RA and IL-13RA1 may contribute to the development of liver fibrosis[32]. In contrast to the conventional decoy receptor hypothesis that often considers IL-13RA2 non-functional, our data reveal its significant upregulation at week 9 post-infection. Notably, the magnitude of this increase surpassed that of both IL-13RA1 and IL-4RA, prompting further investigation. Through functional studies employing both overexpression and knockdown approaches, we demonstrated that IL-13RA2 plays an essential role in the development of *Schistosoma japonicum*-induced liver fibrosis.

Extensive research supports that TGF-β drives tissue fibrosis. TGF-β can induce excessive extracellular matrix and activate fibroblasts *via* the classical SMAD-dependent pathway[33, 34]. Previous studies have shown that IL-13 can drive TGF-β production through IL-13RA2 signaling and promote fibrosis in colitis[35]. Moreover, the CHI3L1-IL-13RA2 complex has been reported to modulate TGF-β1 signaling, regulate antibacterial immune responses, and promote inflammasome activation. [36]. Similarly, in bleomycin-induced pulmonary fibrosis, blocking IL-13RA2 signaling *in vivo* reduces TGF-β expression, as well as pulmonary fibrosis and collagen deposition[37]. However, the regulatory role of IL-13RA2 beyond the TGF-β pathway warrants further investigation. It has been reported that IL-11 promotes lung fibroblasts activation by activating TGF-β1/MEK/ERK signaling[17]. These studies suggest that the TGF-β/MEK/ERK pathway is involved in various fibrotic diseases. However, some studies have suggested that the MEK-ERK signaling pathway can function independently of the classical TGF-β1/SMAD3 pathway and is crucial in promoting cardiac fibrosis[18]. Using the UCSC Gene Interactions tool, we identified the potential interactions between IL-13RA2 and two MAPK pathway genes (*Map2k2*

and *Map2k1*). In our study, the phosphorylation levels of MEK1/2 and ERK1/2 correlated with the expression of IL-13RA2 in mice injected with plasmids overexpressing or silencing *Il13ra2*. Additionally, in JS1 cell lines, IL-13 stimulation, both with and without TGF-β, provided further evidence that IL-13 alone is sufficient to activate the MEK/ERK pathway, even without TGF-β.

IL-13 signaling pathway may alter both the number and composition of immune cells within granulomas, including eosinophils. However, in the present study, we did not perform a detailed quantitative analysis of granuloma-associated cell populations. In addition, data from the Human Protein Atlas indicate that IL-13RA2 is also expressed in hepatocytes and non-parenchymal liver cells, such as liver-resident macrophages (Kupffer cells) and liver sinusoidal endothelial cells. The potential contribution of IL-13RA2 expression in these cell populations to liver fibrosis has not yet been systematically investigated. These aspects represent limitations of the current study and warrant further investigations.

In summary, our study demonstrates that IL-13RA2 expression is markedly induced at week 9 following *Schistosoma japonicum* infection. Both IL-13 overexpression and *Il13ra2* overexpression exacerbate liver fibrosis in schistosomiasis, whereas silencing *Il13ra2* expression partially alleviates fibrotic progression. Moreover, we identified a regulatory role for IL-13RA2 in modulating the MEK/ERK signaling pathway during hepatic fibrogenesis. Collectively, these findings provide new mechanistic insights into IL-13RA2-mediated liver fibrosis and suggest IL-13RA2 as a potential therapeutic target for fibrosis-associated diseases.

Funding

This work was supported by grants from the National Natural Science Foundation of China (Grant Nos. 81 971 965 and 82 472 316) and Jiangsu Provincial Science And Technology Project (Grant No. SBK2024022801).

Acknowledgments

We also thank the Animal Core Facility of Nanjing Medical University for providing laboratory mice.

Author contributions

Ruiyan Xiong: Methodology, Investigation, Data curation, Visualization, Writing —original draft. **Jiangyuan Du:** Investigation, Formal analysis, Validation. **Yuchen Yang:** Formal analysis, Visualization. **Yuxiao Zhu:** Formal analysis, Visualization. **Yangyue Ni:** Methodology. **Lin Chen:** Supervision. **Min Hou:** Supervision. **Zhipeng Xu:** Supervision. **Lu Chen:** Conceptualization, Supervision, Writing—review & editing. **Minjun Ji:** Conceptualization, Project administration, Funding acquisition, Writing—review & editing. All authors read and approved the final version of the manuscript.

References

[1] Kokaliaris C, Garba A, Matuska M, et al. Effect of preventive chemotherapy with praziquantel on schistosomiasis among school-aged children in sub-Saharan Africa: A spatiotemporal modelling study[J]. *Lancet Infect Dis*, 2022, 22(1): 136–149.

[2] Huang J, Yin X, Zhang L, et al. Serum proteomic profiling in patients with advanced *Schistosoma japonicum*-induced hepatic fibrosis[J]. *Parasites Vectors*, 2021, 14(1): 232.

[3] McManus DP, Dunne DW, Sacko M, et al. Schistosomiasis[J]. *Nat Rev Dis Primers*, 2018, 4(1): 13.

[4] Zhang Y, Li J, Li H, et al. A preliminary investigation into the immune cell landscape of schistosome-associated liver fibrosis in humans[J]. *Immunol Cell Biol*, 2021, 99(8): 803–813.

[5] Ding T, Ge S. Metabolic regulation of type 2 immune response during tissue repair and regeneration[J]. *J Leukoc Biol*, 2022, 112(5): 1013–1023.

[6] Abdel Aziz N, Musaigwa F, Mosala P, et al. Type 2 immunity: A two-edged sword in schistosomiasis immunopathology[J]. *Trends Immunol*, 2022, 43(8): 657–673.

[7] Song LJ, Yin XR, Mu SS, et al. The differential and dynamic progression of hepatic inflammation and immune responses during liver fibrosis induced by *Schistosoma japonicum* or carbon tetrachloride in mice[J]. *Front Immunol*, 2020, 11: 570524.

[8] Wang Z, Du K, Jin N, et al. Macrophage in liver Fibrosis: Identities and mechanisms[J]. *Int Immunopharmacol*, 2023, 120: 110357.

[9] Hammerich L, Tacke F. Hepatic inflammatory responses in liver fibrosis[J]. *Nat Rev Gastroenterol Hepatol*, 2023, 20(10): 633–646.

[10] Rahaman SO, Sharma P, Harbor PC, et al. IL-13Rα2, a decoy receptor for IL-13 acts as an inhibitor of IL-4-dependent signal transduction in glioblastoma cells[J]. *Cancer Res*, 2002, 62(4): 1103–1109.

[11] Daines MO, Hershey GKK. A novel mechanism by which interferon-γ can regulate interleukin (IL)-13 responses: Evidence for intracellular stores of IL-13 receptor α-2 and their rapid mobilization by interferon-γ[J]. *J Biol Chem*,

2002, 277(12): 10387–10393.

[12] Zhao X, Yang W, Yu T, et al. Th17 cell-derived amphiregulin promotes colitis-associated intestinal fibrosis through activation of mTOR and MEK in intestinal myofibroblasts[J]. *Gastroenterology*, 2023, 164(1): 89–102.

[13] Lumsden RV, Worrell JC, Boylan D, et al. Modulation of pulmonary fibrosis by IL-13Rα2[J]. *Am J Physiol Lung Cell Mol Physiol*, 2015, 308(7): L710–L718.

[14] Ullah R, Yin Q, Snell AH, et al. RAF-MEK-ERK pathway in cancer evolution and treatment[J]. *Semin Cancer Biol*, 2022, 85: 123–154.

[15] Wang X, Lu Y, Wu L, et al. Moxibustion inhibits the ERK signaling pathway and intestinal fibrosis in rats with Crohn's disease[J]. *Evid Based Complement Alternat Med*, 2013, 2013(1): 198282.

[16] Han C, Wu X, Zou N, et al. *Cichorium pumilum* Jacq extract inhibits LPS-induced inflammation via MAPK signaling pathway and protects rats from hepatic fibrosis caused by abnormalities in the gut-liver axis[J]. *Front Pharmacol*, 2021, 12: 683613.

[17] Chen H, Chen H, Liang J, et al. TGF-β1/IL-11/MEK/ERK signaling mediates senescence-associated pulmonary fibrosis in a stress-induced premature senescence model of *Bmi-1* deficiency[J]. *Exp Mol Med*, 2020, 52(1): 130–151.

[18] Umbarkar P, Tousif S, Singh AP, et al. Fibroblast GSK-3α promotes fibrosis via RAF-MEK-ERK pathway in the injured heart[J]. *Circ Res*, 2022, 131(7): 620–636.

[19] Mawa PA, Kincaid-Smith J, Tukahebwa EM, et al. Schistosomiasis morbidity hotspots: Roles of the human host, the parasite and their interface in the development of severe morbidity[J]. *Front Immunol*, 2021, 12: 635869.

[20] Buonfrate D, Ferrari TCA, Adegnika AA, et al. Human schistosomiasis[J]. *Lancet*, 2025, 405(10479): 658–670.

[21] Gieseck III RL, Wilson MS, Wynn TA. Type 2 immunity in tissue repair and fibrosis[J]. *Nat Rev Immunol*, 2018, 18(1): 62–76.

[22] Allen JE. IL-4 and IL-13: Regulators and effectors of wound repair[J]. *Annu Rev Immunol*, 2023, 41(1): 229–254.

[23] Beschin A, De Baetselier P, Van Ginderachter JA. Contribution of myeloid cell subsets to liver fibrosis in parasite infection[J]. *J Pathol*, 2013, 229(2): 186–197.

[24] Reißing J, Berres M, Strnad P, et al. Th2 cell activation in chronic liver disease is driven by local IL33 and contributes to IL13-dependent fibrogenesis[J]. *Cell Mol Gastroenterol Hepatol*, 2024, 17(4): 517–538.

[25] Fallon PG, Richardson EJ, McKenzie GJ, et al. Schistosome infection of transgenic mice defines distinct and contrasting pathogenic roles for IL-4 and IL-13: IL-13 is a profibrotic agent[J]. *J Immunol*, 2000, 164(5): 2585–2591.

[26] Vicentino ARR, Carneiro VC, Allonso D, et al. Emerging role of HMGB1 in the pathogenesis of schistosomiasis liver fibrosis[J]. *Front Immunol*, 2018, 9: 1979.

[27] Yombo DJK, Odayar V, Gupta N, et al. The protective effects of IL-31RA deficiency during bleomycin-induced pulmonary fibrosis[J]. *Front Immunol*, 2021, 12: 645717.

[28] Melo-Cardenas J, Bezavada L, Crawford JC, et al. IL-13/IL-4 signaling contributes to fibrotic progression of the myeloproliferative neoplasms[J]. *Blood*, 2022, 140(26): 2805–2817.

[29] Junttila IS. Tuning the cytokine responses: An update on interleukin (IL)-4 and IL-13 receptor complexes[J]. *Front Immunol*, 2018, 9: 888.

[30] Vannella KM, Barron L, Borthwick LA, et al. Incomplete deletion of IL-4Rα by $LysM^{Cre}$ reveals distinct subsets of M2 macrophages controlling inflammation and fibrosis in chronic schistosomiasis[J]. *PLoS Pathog*, 2014, 10(9): e1004372.

[31] Weng SY, Wang X, Vijayan S, et al. IL-4 receptor alpha signaling through macrophages differentially regulates liver fibrosis progression and reversal[J]. *EBioMedicine*, 2018, 29: 92–103.

[32] Adhyatmika A, Putri KSS, Gore E, et al. Osteoprotegerin expression in liver is induced by IL13 through TGFβ[J]. *Cell Physiol Biochem*, 2022, 56(1): 28–38.

[33] Meng XM, Nikolic-Paterson DJ, Lan HY. TGF-β: The master regulator of fibrosis[J]. *Nat Rev Nephrol*, 2016, 12(6): 325–338.

[34] Liu J, Kong D, Qiu J, et al. Praziquantel ameliorates CCl_4-induced liver fibrosis in mice by inhibiting TGF-β/Smad signalling via up-regulating Smad7 in hepatic stellate cells[J]. *Br J Pharmacol*, 2019, 176(24): 4666–4680.

[35] Fichtner-Feigl S, Young CA, Kitani A, et al. IL-13 signaling via IL-13$R\alpha_2$ induces major downstream fibrogenic factors mediating fibrosis in chronic TNBS colitis[J]. *Gastroenterology*, 2008, 135(6): 2003–2013. e7.

[36] He CH, Lee CG, Dela Cruz CS, et al. Chitinase 3-like 1 regulates cellular and tissue responses via IL-13 receptor α2[J]. *Cell Rep*, 2013, 4(4): 830–841.

[37] Mentink-Kane MM, Wynn TA. Opposing roles for IL-13 and IL-13 receptor α2 in health and disease[J]. *Immunol Rev*, 2004, 202(1): 191–202.